A SPECTRAL FUNCTION METHOD APPLIED TO THE CALCULATION OF THE WAKE FUNCTION FOR THE NLCTA

R.M. Jones[†‡], K. Ko[†], N.M. Kroll[†‡] and R.H. Miller[†]

†Stanford Linear Accelerator Center, M/S 26, P.O Box 4349, Stanford, CA 94309

‡University of California, San Diego, La Jolla, CA 92093-0319.

Abstract

The sum over damped modes, which provides the main contribution to the transverse wake of the DDS, is replaced by a Fourier-like integral of a spectral function over the propagation band of the manifolds. We present comparisons to previous calculations, assessment of appropriate domains of applicability, and applications to the SLAC structure with matched and mismatched manifold terminations.

1. Introduction

The recently completed prototype accelerating cavity for the NLCTA incorporates both damping and detuning (the DDS structure) of the higher order modes (HOM), with the objective of suppressing the transverse wakefield experienced by trailing bunches [1,2]. The current analysis of the structure is based upon an equivalent circuit model whose current form is described in [1]. We use the Bane-Gluckstern two band model [3], extended to include the damping manifold. The latter is represented by a rectangular TE_{10} waveguide mode, periodically shunted with a series LC circuit, with the shunt capacitively coupled to the TE component of the two band model. Each section of the structure is described by nine circuit parameters defined and determined as described in [1] along with the beam coupling parameters (cell kick factors [3]). In the following sections we the explain the the spectral function method, and compare it to our previous methods. The spectral function method is then applied to compute the dependence of the wake function on the manifold terminations.

2. Review of the Fundamentals of the Wake Function Calculation

The TE and TM cell excitation amplitudes are related to the drive beam via the circuit equations. In matrix form and in the frequency domain this relation takes the form:

$$\begin{pmatrix} \hat{H} & H_x^t \\ H_x & H - GR^{-1}G \end{pmatrix}\begin{pmatrix} \hat{a} \\ a \end{pmatrix} - f^{-2}\begin{pmatrix} \hat{a} \\ a \end{pmatrix} = f^{-2}\begin{pmatrix} B \\ 0 \end{pmatrix} \quad (1)$$

where the quantities in the above expression are defined in [1]. The elements in the above 2 by 2 matrix are themselves N by N matrices, where N is the number of cells. $\hat{H}$ and H are tridiagonal matrices which describe the coupled chains of TM and TE resonant circuits, while H_x is the tridiagonal matrix with vanishing diagonal elements which describes the

TE-TM coupling. R, which describes the manifold, is also tridiagonal, while G, which describes the coupling of the TE chain to the manifold, is diagonal. The diagonal elements of H, G, and R are frequency dependent. Corresponding to the above, each element of the column vectors are themselves N element vectors. To further condense the notation we may also write Eq. (1) in 2N by 2N matrix form

$$\overline{H}\overline{a} - f^{-2}\overline{a} = f^{-2}\overline{B} \quad (2)$$

The drive beam, represented by the N component vector B, couples only to the TM mode. We take it to be a point charge moving at velocity c and normalize it per unit charge per unit displacement. With this understanding it takes the form

$$B_n = \sqrt{(4\pi f_s^n / c)K_s^n L} \, \exp[-(j2\pi f / c)n] \quad (3)$$

where L is the periodicity length, K_s^n the Bane-Gluckstern kick factor evaluated at the synchronous mode and f_s^n the synchronous mode frequency, both evaluated for a uniform structure based upon the n'th cell [3]. The transverse wake-function (ie wake potential per unit length) for a particle trailing a distance s behind a velocity c drive bunch (per unit drive bunch charge per unit drive bunch displacement) may be written

$$W(s) = \int [Z(f - j\varepsilon)\exp[(2\pi j s / c)(f - j\varepsilon)]df \quad (4)$$

where ε is a positive infinitesimal quantity and the wake impedance Z is given by

$$Z(f) = \pi^{-1}\sum_{n,m}^{N} \sqrt{K_s^n K_s^m f_s^n f_s^m} \, \exp[(2\pi jL / c)f(n - m)]\tilde{H}_{nm} \quad (5)$$

with the 2N by 2N matrix $\tilde{H}$ given by

$$\tilde{H} = \overline{H}(1 - f^{-2}\overline{H})^{-1} \quad (6)$$

From causality Z(f) can be analytically extended to the LHP, and singularities on the real axis are avoided in Eq. (4) by integration over f just below the real axis as indicated in Eq. (4). Because W is real, we also have Z(f) = Z*(-f*), for f in the LHP. Because Z is real for sufficiently low frequencies on the real axis, Z*(f*) provides an analytic extension of Z into the UHP. Since the Z so defined is discontinuous across the real axis where Z is complex, cuts are introduced there to

render Z single valued on what we call the "physical sheet" of its Riemann surface. It also satisfies $Z(f) = Z(-f)$, that is, it is an even function of f in the complex plane. We note that Z is actually a four valued function arising from the sign ambiguity in $\sin\phi_1$ and $\sin\phi_N$, quantities which appear in R_{11} and R_{NN} respectively [1]. (The $\cos\phi_n$, defined by Eq. (4) of [1] are single valued analytic functions, but the corresponding sines are defined only by the trigonometric identity, $\sin^2 + \cos^2 = 1$.) Damped modes appear as complex poles on sheets of the Riemann surface adjacent to the physical sheet.

3. The Spectral Function Method for Computing the Wake Function

Because the equivalent circuit wake function contains a small non-physical precursor on the [-NL,0] interval [3], it proves to be convenient to define a "causal" wake function by

$$W_c(s) = \theta(s)[W(s) - W(-s)] \tag{7}$$

W_c equals W for s > NL and vanishes for negative s. In the interval [0,NL] W(-s) would be zero in the absence of a precursor. Hence Eq. (7) represents a smooth way of suppressing the precursor, and W_c is more likely to portray the actual structure than the strict equivalent circuit model. From Eq. (4) and the symmetry properties of Z noted in the previous section we have

$$W(-s) = \int_{-\infty}^{\infty} Z(f + j\varepsilon)\exp[(2\pi js/c)(f + j\varepsilon)]df \tag{8}$$

which leads to

$$W(s) - W(-s) = 2j\int_{-\infty}^{\infty} \mathrm{Im}\{Z(f - j\varepsilon)\}\exp[(2\pi js/c)f]df \tag{9}$$

$$= 4\int_{0}^{\infty} \mathrm{Im}\{Z(f + j\varepsilon)\}\sin[(2\pi js/c)f]df \tag{10}$$

To include the contribution of poles on the real axis (with real residue) in Eqs. (9) and (10) we interpret

$$\mathrm{Im}\{(f \pm j\varepsilon - f_0)^{-1}\} = \mp\pi\delta(f - f_0) \tag{11}$$

and define $4\mathrm{Im}\{Z(f+j\varepsilon)\}$ as the spectral function S(f) of the wake function. Thus we have

$$W_c(s) = \theta(s)\int_{0}^{\infty} S(f)\sin[(2\pi s/c)f]df \tag{12}$$

We note further that the usually displayed wake envelope function $\hat{W}(s)$ associated with W_c is given by

$$W_c(s) = \theta(s)\left|\int_{0}^{\infty} S(f)\exp[(2\pi s/c)f]df\right| \tag{13}$$

For the undamped case, which in the context of the NLCTA design is obtained by setting the coupling matrix G to zero, Z is real on the real axis and contains a set of poles on the real axis at the modal frequencies. The spectral function is then simply a sum of delta functions:

$$S(f) = 2\sum_{p} K_p\delta(f - f_p) = 2K_n dn/df \tag{14}$$

where the f_p are the modal frequencies, n(f) is the number of modes with frequency less than f, and the K_p are called modal kick factors. The spectral function and the modal sum methods are thus formally identical. In the presence of damping, Z is complex on those portions of the real axis which lie in the propagation bands of the manifolds, and poles which would lie on that portion of the real axis in the absence of coupling to the manifold split into complex conjugate pairs on the non-physical sheets accessed by analytic continuation through the cuts. When the coupling is weak so that their position can be found by perturbation theory, their distance from the real axis is small compared to their separation, and the spectral function has sharp narrow peaks in place of the delta functions of the undamped case. As the coupling strength increases these poles move further from the real axis, the peaks broaden, and while the peaks generally remain quite discernable, the behaviour is relatively smooth. The spectral function can be computed as a function of frequency by direct evaluation of Eq. (5). A combination of an N by N matrix inversion and the solution of a 2N system of linear equations is involved. In the weak coupling case it is relatively simple to determine the modal frequencies, eigenvectors and Q values and hence to compute the damped modal sum. In contrast a large number of frequency points is required to adequately delineate the narrow peaked spectral function. The situation is reversed in the strong coupling case. The process of determining the modes has proved to be quite difficult and computer time consuming [1], while on the other hand the number of frequency points required to adequately describe the more smoothly varying spectral function becomes more reasonable. The wake functions computed from the modal expansion and from the spectral function have been compared for the single example of the former which has been carried out and found to be in excellent agreement [4].

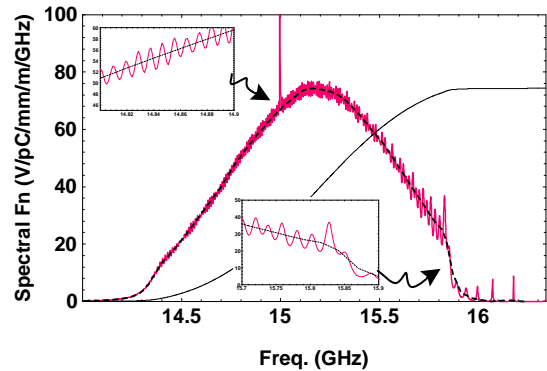### 4. Applications of the Spectral Function Method

Fig 1: Spectral Function and integral for Matched HOM Coupler and $2K\delta n/\delta f$ (Shown Dashed)

The spectral function method has so far been employed principally to explore the effect of manifold mismatch on the DDS wake function. We begin with the spectral function for the matched manifold case, shown in Fig. 1. We have shown the smoothed spectral function, $2K_n\delta n/\delta f$, for the undamped case (ie the G set equal to zero case) on the same curve. (The unsmoothed spectral function, $2K_n dn/df$, is a sum of delta functions as noted before.) One sees that the effect of the damping is to replace the delta functions by broadened peaks which produce an oscillation about the smoothed umdamped spectral function. The wake envelope function for the matched DDS structure and, for comparison, the corresponding function for the NLCTA DT structure are shown in [5]. There the recoherance peak of the DT is seen to be strongly suppressed by the damping.
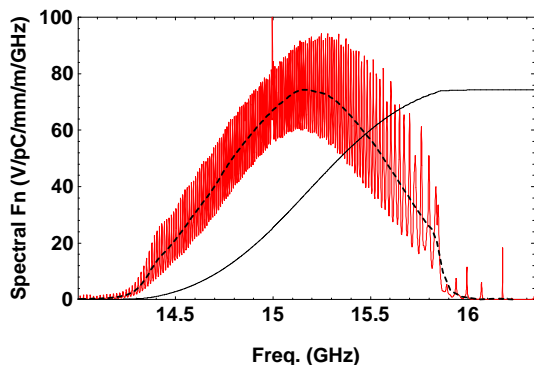

Fig 2: Spectral Function For Fabricated DDS and its Integral

A series of investigations demonstrated that the wake function was seriously degraded by small mismatches of the manifolds, especially on the output (hence downtapered) side. Accordingly a major effort was made to design mitered bend type structures to match the manifolds to standard waveguide (WR62 was used). The results achieved for both the input and output side are given in [4]. In order to test the structure in the ASSET experiment it is necessary to attach windows and loads. The available windows were unfortunately not well-matched in the 14 to 16 GHz band that is crucial to the damping. The window and manifold added
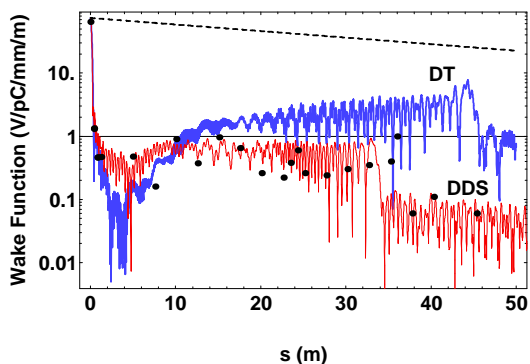

Figure 3: Wake Function for Fabricated DDS, ASSET data for DDS and NLCTA DT (Copper Losses Shown Dashed)

in quadrature are also illustrated in [6]. The combined reflection coefficient for the output end of the manifold has a minimum of .09 at 15.05 GHz rising to .37 at 14.2 and .4 at 16. Ghz. At the input end the reflection coefficients are similar in the upper half of the frequency range but less than .09 for the lower half.

The effect of these reflections on the spectral function and wake envelope function are shown in Figs. 2 and 3. As compared to the matched case the oscillations of the spectral function show a large increase in amplitude, indicating significantly higher Qs for many of the modes, and the wake envelope function is substantially degraded. However, even with the degradation shown in Fig. 3, the results constitute a considerable improvement over the DT structure. Preliminary ASSET experimental results have already been obtained [7], and the experimental points have been superposed on the Fig. 3 curve. Matched windows over the required band are in preparation, and simulations already performed [4] indicate a two-fold improvement in the wake function over that of the present structure.

5. Conclusion

The DDS described here was designed with rather crude theoretical tools [2]. However, the well-founded theoretical analysis given here and in [1] were carried out after the design was complete (but prior to fabrication). While the agreement between the preliminary experimental results and the theoretical predictions is imperfect, given the differences (some planned, some inadvertant) between the theoretical design and the structure as fabricated, the comparison suggests that the present version of the theory provides both the physical insight and the quantitative analysis needed to design an improved structure, and a number of such improvements are under consideration [4].

6. Acknowledgments

7. References

[1] R.M. Jones, et al, Equivalent Circuit Analysis of The SLAC Damped Detuned Structure, SLAC-PUB-7187, EPAC96 Proc.
[2] K. Ko, et al, Design Parameters for the Damped Detuned Accelerating Structure, SLAC-PUB-95-6844, PAC95 Proc.
[3] K. Bane and R. Gluckstern, Particle Accls.,42, p 123 (1993).
[4] R.M. Jones et al, 1996, To be submitted, Phys, Rev E.
[5] R.H. Miller, et al, A Damped Detuned Structure for the Next Linear Collider. Paper Thp02 in this conference.
[6] M. Seidel, et al, Microwave Analysis of the Damped Detuned Structure. Paper Thp05 in this conference.
[7] C. Adolphson, et al, Aug. '96, private communication.